# Features of Isoforms of Human Soluble TACI

**Miriam L. Fichtner,[*,†] Heike Rübsamen,[*,†] Michaela Smolle,[‡,§] Jonas Schaller,[*,†] Regina Feederle,[¶] Andreas Bültmann,[‖] Tania Kümpfel,[*,†] Pascal Schneider,[#] Franziska S. Thaler,[*,†,**,1] and Edgar Meinl[*,†,1]**

**The BAFF/APRIL-system with the two cytokines BAFF and APRIL and their three receptors, transmembrane activator and CAML interactor (TACI), BAFF receptor, and B-cell maturation Ag, is important for B cell maintenance. The BAFF/APRIL system is a therapeutic target in B cell–derived malignancies and autoimmune diseases. However, unexpected outcomes of clinical trials with atacicept (TACI-Fc) underline our incomplete understanding of this system. Shedding of the three receptors is one important regulatory element. In humans, TACI exists in two isoforms generated through alternative splicing in their extracellular portion: TACI-long (l) has two cysteine-rich domains, whereas TACI-short (s) lacks the first low-affinity one. In this study, we discriminated soluble (s) forms of TACI-l and TACI-s with newly generated mAbs and found that both were spontaneously released from activated human B cells, with a predominance of sTACI-l. Furthermore, sTACI-l was also the dominant isoform in human serum. Vaccination with the mRNA vaccine from BioNTech does not significantly affect the serum levels of sTACI-l. Both TACI-s and TACI-l were shed by a disintegrin and metalloproteinase domain-containing protein 10. TACI-l and TACI-s formed homo- and hetero-oligomers in soluble and membrane-bound forms. Both sTACI-l and sTACI-s acted as decoy receptors for BAFF, but only sTACI-l also efficiently inhibited APRIL. Dimerization of sTACI-l enhanced its decoy functions only slightly. Together, we extend our knowledge of the complexity of the BAFF/APRIL system by identifying and characterizing the two soluble isoforms of TACI.** ***The Journal of Immunology*****, 2023, 211: 1–10.**

The BAFF/APRIL-system plays a crucial role in the development and maintenance of B cells (1, 2). It is composed of the two ligands BAFF and APRIL and the three receptors, BAFF receptor (BAFF-R), B-cell maturation Ag (BCMA), and transmembrane activator and CAML interactor (TACI).

The importance of this system is further substantiated by its proven value as a therapeutic target in autoimmune diseases and hemato-oncology (3, 4): belimumab (anti-BAFF) is used to treat patients with systemic lupus erythematosus (3). mAbs targeting BCMA and chimeric Ag receptor (CAR)-T cells targeting BCMA and/or TACI raised great hope as novel therapeutic strategies against multiple myeloma (4–9). Recently, belantamab mafodotin (GSK28579176), an anti-BCMA drug conjugate, and CAR-T cells targeting BCMA have been approved for the treatment of multiple myeloma (reviewed in [10]). One pharmacological approach to target both BAFF and APRIL is the application of atacicept (TACI-Fc, comprising both cysteine-rich domains [CRDs] of TACI). Atacicept reduced circulating Ig levels, as expected, because BAFF and APRIL are survival factors for plasma cells. Atacicept also reduced the total number of circulating B cells but not of memory B cells. Unexpectedly, atacicept induced inflammatory activity in the brain of some patients with multiple sclerosis (MS), and the clinical trial was stopped (11). The reasons behind this are still not understood but may partially be explained by observations that BAFF and APRIL foster immunoregulatory activity of plasmablasts (12–14) and astrocytes (15). This illustrates that features of the powerful regulatory BAFF/APRIL system remain to be explored.

This study focuses on TACI. Surface expression of TACI is induced when B cells are activated, in particular when they differentiate into plasma cells (16, 17); TACI is also expressed by malignant cells such as in primary CNS lymphoma (18) and multiple myeloma (19). The surface receptor TACI binds to both BAFF and APRIL but responds better, if not exclusively, to oligomeric ligands (i.e., containing more than one trimer: membrane-bound BAFF, BAFF 60-mer [containing 20 trimers], or heparan sulfate proteoglycan-bound APRIL) (1, 20). Mutations of TACI are a cause of common variable immunodeficiency (21). Some of these patients showed signs of lymphoproliferation and autoimmunity together with immunodeficiency (22), illustrating the complex role of TACI.

*Institute of Clinical Neuroimmunology, University Hospital, LMU Munich, Munich, Germany; [†]Biomedical Center, Faculty of Medicine, LMU Munich, Martinsried, Germany; [‡]Physiological Chemistry, Biomedical Center, LMU Munich, Martinsried, Germany; [§]BioPhysics Core Facility, Biomedical Center, LMU Munich, Martinsried, Germany; [¶]Monoclonal Antibody Core Facility, Helmholtz Zentrum München, German Research Center for Environmental Health, Neuherberg, Germany; [‖]MorphoSys AG, Planegg, Germany; [#]Department of Immunobiology, University of Lausanne, Lausanne, Switzerland; and **Munich Cluster for Systems Neurology (SyNergy), Munich, Germany

[1]F.S.T. and E.M. contributed equally to this work.

ORCIDs: 0000-0001-8900-1541 (M.S.); 0000-0002-3981-367X (R.F.); 0009-0002-4443-8904 (A.B.); 0000-0003-0677-9409 (P.S.); 0000-0002-2570-6785 (E.M.).

Received for publication November 22, 2021. Accepted for publication May 4, 2023.

This work was supported by the Deutsche Forschungsgemeinschaft (SFB-TR128), Merck (GMSI award 2018 to E.M.), Novartis Pharma, the Gemeinnützige Hertie Stiftung, the Else-Kröner Fresenius Stiftung, and the Munich Cluster for Systems Neurology (SyNergy). P.S. is supported by the Swiss National Science Foundation (grant 310030-205196). M.L.F. was supported through a Deutsche Forschungsgemeinschaft research fellowship (FI 2471/1-1, FI 2471/2-1).

Address correspondence and reprint requests to Prof. Edgar Meinl, Institute of Clinical Neuroimmunology, Biomedical Center, Ludwig-Maximilians-Universität München, Großhaderner Strasse 9, 82152 Planegg-Martinsried, Germany. E-mail address: edgar.meinl@med.uni-muenchen.de

The online version of this article contains supplemental material.

Abbreviations used in this article: ADAM10, a disintegrin and metalloproteinase domain-containing protein 10; APRIL, a proliferation-inducing ligand; ATCC, American Type Culture Collection; BAFF, B-cell activating factor; BAFF-R, BAFF receptor; BCMA, B-cell maturation Ag; CAR, chimeric Ag receptor; co-IP, coimmunoprecipitation; CRD, cysteine-rich domain; DAPT, (2S)-N-[(3,5-Difluorophenyl)acetyl]-L-alanyl-2-phenyl] glycine 1,1-dimethylethyl ester; MS, multiple sclerosis; RT, room temperature; s, soluble; SEC, size exclusion chromatography; sTACI, soluble transmembrane activator and CAML interactor; TACI, transmembrane activator and CAML interactor; TACI-l, TACI-long; TACI-s, TACI-short.

In humans, but not in mice, the *TNFRSF13B* gene generates two alternative splicing variants of TACI (23). The short splice variant TACI-short (s) lacks the N-terminal CRD1 but retains the CRD2. The CRD2 of TACI was found to be sufficient for ligand binding (23), whereas the CRD1 was implicated in oligomerization of TACI in membrane-bound form (24). In recent years, a further level of regulation within the BAFF/APRIL system has been identified, namely shedding of the three receptors BCMA (25), TACI (17), and BAFF-R (26), reviewed in (27). Soluble (s)BCMA and sTACI are biomarkers for B cell involvement in autoimmunity and lymphoma and have to be considered in therapeutic approaches targeting these receptors (17, 18, 25, 28, 29).

Although the membrane-bound isoforms of TACI have been linked to the induction of plasma cell differentiation (30, 31), properties of their respective shed forms (sTACI-l and sTACI-s) have not been investigated and are the focus of this study. Using isoform-specific mAbs to differentiate between sTACI-s and sTACI-l, we found that both sTACI isoforms were spontaneously shed from activated human B cells. The levels of sTACI-l were ∼10 times higher than the levels of sTACI-s. In serum, sTACI-l was the dominant isoform, and the levels did not significantly change after vaccination with the mRNA vaccine from BioNTech. Furthermore, we found that sTACI-s was not shed by γ-secretase like BCMA was, although both receptors have just one CRD. sTACI-l and sTACI-s showed differences in their degree of oligomerization and decoy activity. Thus, this study extends our knowledge of the complexity of the BAFF/APRIL system.

## Materials and Methods

### *Human specimen*

All human specimens were collected following written informed consent according to local ethics policy guidelines at the Ludwig Maximilian University in Munich. This study abides by the Declaration of Helsinki principles. Written informed consent was obtained from each donor prior to their inclusion in the study. Characteristics and demographics on the healthy control subjects and the donors can be found in Supplemental Table I.

### *Recombinant production of sTACI-l and sTACI-s*

Sequences of mature soluble TACI isoforms cloned in expression vectors were chosen according to mass spectrometry results published in (17). sTACI-l (*DAA*MSGLGRSRRGGRSRVDQEERFPQGLWTGVAMRSCPEEQYWDPLLGTCMSCKTICNHQSQRTCAAFCRSLSCRKEQGKFYDHLLRDCISCASICGQHPKQCAYFCENKLRSPVNLPPELRRQRSGEVENNSDNSGRYQGLEHRGSEASPALPGLK*HHHHHH*) and sTACI-s (*DAA*MSGLGRSRRGGRSRVDQEERWSLSCRKEQGKFYDHLLRDCISCASICGQHPKQCAYFCENKLRSPVNLPPELRRQRSGEVENNSDNSGRYQGLEHRGSEASPALPGLK*HHHHH*), where sequences in italic are vector derived, were produced in HEK293.EBNA cells using the PTT5 vector essentially as described previously (25, 32). We chose K154 of TACI-l (K108 of TACI-s), adjacent to L155, as the mature C-terminus of the recombinant proteins because K154/L155 within the juxtamembrane region is close to the natural cleavage site of naturally processed sTACI (17). Because TACI is devoid of a signal peptide, the signal peptide of the Ig κ-chain was added at the N-terminus of sTACI-l and sTACI-s to ensure secretion. A tag coding for six consecutive histidines was added at the C-terminus for affinity purification purposes. Proteins secreted in serum-free conditioned supernatants of transfected HEK293.EBNA cells were affinity purified by nickel-nitriloacetic acid affinity chromatography with HisTrap columns (GE Healthcare) and a gradient using imidazole. Details of recombinant sTACI-s and sTACI-l are provided in Fig. 1.

### *SDS-PAGE, Coomassie blue staining, and Western blotting*

Proteins were denatured for SDS-PAGE by heating for 5 min at 95°C in NuPAGE sample buffer with 50 mM DTT. Novex Bis-Tris gels (6–12%; Invitrogen) or Novex Tricine 10–20% gels (Invitrogen) and Novex sharp prestained protein standard (Thermo Scientific) were used for SDS-PAGE. After electrophoresis, gels were stained with Coomassie blue. Analysis was done by Odyssey Fc (LI-COR Biosciences) with 700 nm.

### *Generation and characterization of mAbs recognizing sTACI-l and sTACI-s*

Several mAbs were produced to distinguish both isoforms of human TACI. mAbs that specifically recognize the long isoform were generated by MORPHOSYS using a phage display library in a human IgG1 format (33). TACI-s is characterized by Trp21 that is generated by alternative splicing. For Abs specifically recognizing TACI-s, rats were immunized twice with an OVA-coupled peptide, DQEERWSLSCR, containing Trp21 coupled to OVA. Hybridoma fusion was performed using standard procedures, and supernatants from the obtained clones were first screened for binding to biotinylated peptides by ELISA. Positive clones were then further validated with recombinant sTACI-s and sTACI-l by ELISA and Western blot analysis. Selected clones were subcloned by limiting dilution to generate monoclonal hybridoma cell lines. Furthermore, the commercially available mAb CD267 (TACI) mAb (clone 11H3 (biotinylated); 13-9217-82, Invitrogen) is specific for sTACI-l (31). 11H3, one TACI-l-specific mAb from phage display (B10), and the new TACI-s specific mAb (9C5, rat IgG2b) were chosen for this study.

### *ELISAs*

The human TACI/TNFRSF13B DuoSet ELISA (DY174, R&D Systems, Abingdon, UK) detects both isoforms of TACI and was used to detect total sTACI. TACI isoform-specific ELISAs were established. The TACI-s–specific mAb 9C5 and the TACI-l–specific mAb B10 were used as capture Abs. Both Abs were coated in ELISA plates at a concentration of 5 μg/ml and incubated overnight at 4°C. Recombinant human sTACI-s and sTACI-l were used as standards to determine sample concentration. Samples were incubated for 2 h at room temperature (RT) for validation of the mAbs and sTACI-l. The biotinylated goat anti-human TACI (841862, R&D Systems), followed by HRP-coupled streptavidin (DY998, R&D Systems) and substrate solution (DY999, R&D Systems), was used for subsequent detection. We established another ELISA specific for sTACI-l by coating with the anti-TACI Ab [Human TACI Capture Ab (841861, R&D Systems)] and detected with 11H3-biotin. The sensitivity of sTACI-s detection could be increased by incubating samples overnight.

A sandwich ELISA was used to detect binding of sTACI to BAFF and APRIL as previously published (17). In short, ELISA plates were coated overnight at 4°C with anti-Flag M2 Ab (5 μg/ml; Sigma-Aldrich, St. Louis, MO). Human Flag-BAFF (R&D Systems) or mouse Flag-APRIL (AdipoGen) were added at a concentration of 100 ng/ml and incubated for 2 h at RT. Next, a dilution series of the sTACI isoforms (0.0024–37.5 nM, corresponding to ∼0.04–675 ng/ml [sTACI-l]) were added to the ELISA and incubated for 2 h at RT. After washing, the TACI DuoSet ELISA protocol was followed starting with the detection step. Absorbance at 450 nm and 540 nm was measured with the PerkinElmer Victor2 1420 Multilabel Counter.

### *Coimmunoprecipitation (co-IP)*

HEK293T cells were transfected in 10-cm plates using Lipofectamine 2000 (Invitrogen) with plasmids coding for TACI-l or TACI-s tagged at the N-terminus with Flag or HA. Supernatants were harvested, and cell lysates were obtained 48–72 h after transfection. Cells were lysed on ice for 30 min in 1.8 ml lysis buffer (0.5% Nonidet P-40 [Sigma-Aldrich], 50 mM HEPES buffer [Sigma-Aldrich], 250 mM NaCl, 5 mM EDTA [Sigma-Aldrich], Complete protease inhibitor mixture [Sigma-Aldrich]). Lysates were centrifuged once for 10 min at 14,000 rpm, and supernatants were stored at −80°C. The TACI Human TACI/TNFRSF13B DuoSet ELISA (R&D Systems) was used to determine TACI concentrations before addition of beads. Co-IP was performed as previously described (17). Briefly, equal amounts of protein were added stepwise to anti-Flag M2 magnetic beads (M8823; Sigma-Aldrich) for all supernatant conditions to determine oligomerization of soluble TACI isoforms and for all cell lysate conditions to determine oligomerization of membrane-bound forms. After sample application, beads were washed five times with TBS (10 mM Tris-HCl, 140 mM NaCl). Proteins were eluted by incubation with 1 M glycine-HCl, pH 3, for 20 min at 56°C, and supernatants were neutralized with 1 M Tris-HCl, pH 9. Anti-Flag and anti-HA ELISAs were used to quantify immunoprecipitated Flag-TACI and coimmunoprecipitated HA-TACI in bead eluates. Briefly, ELISA plates were coated overnight at 4°C with anti-Flag M2 Ab or anti-HA.11 Ab (HA-7; BioLegend) at 5 μg/ml in PBS. Next, plates were blocked with PBS with 1% BSA, and eluates were incubated for 2 h at RT on anti-HA-coated plates. After washing, the TACI DuoSet ELISA protocol was followed starting with the detection step. Absorbance at 450 nm and 540 nm was measured with the Perkin Elmer Victor2 1420 Multilabel Counter.

### *Size exclusion chromatography (SEC)*

Freshly produced proteins were concentrated to ~3–10 mg/ml with Amicon Ultra centrifugal filters (ULTRACEL-3K). SEC was performed on an ÄKTA PURE chromatography system (GE Healthcare) equipped with online UV monitoring at 280 nm equilibrated and developed in PBS.

### *Mass spectrometry and N-terminal sequencing*

Bands of interest were cut from a Coomassie blue–stained SDS-PAGE gel and digested with trypsin (Serva). The N-terminal parts of the proteins were analyzed by N-terminal sequencing. After running the proteins through gel electrophoresis, the proteins were transferred semidry to a polyvinylidene difluoride membrane. The membrane was consecutively stained for 3–4 min with Coomassie brilliant blue, destained with destaining solution (50% methanol, 7% acetic acid) for 10 min, and washed for 10 min with distilled water. After cutting the bands of interest, the bands were air dried and analyzed using a MALDI-TOF/TOF 4800 Analyzer (Applied Biosystems).

### *NF-κB reporter assay*

The NF-κB assay was performed essentially as previously published (17). HEK293T cells were transfected with the firefly luciferase reporter plasmid, an internal control CMV Renilla luciferase plasmid, and BCMA plasmid. Mouse APRIL (AdipoGen) or BAFF (R&D Systems) was added to a dilution series of sTACI-l or sTACI-s (0.0024–37.5 nM) at a concentration of 100 ng/ml (~3 nM) 8 h after transfection. The sTACI + ligand mixture was incubated at 37°C for 30 min and then added to the transfected cells. NF-κB activation was measured 17 h later. Cells were lysed with passive lysis buffer from Promega. To detect the reporter proteins, a substrate mix of luciferin and ATP (Biozym Scientific GmbH) was used for firefly luciferase and coelenterazine (Promega) for Renilla luciferase. Luminescence was monitored with the PerkinElmer Victor2 1420 Multilabel Counter.

### *Cell culture and analysis of shedding using enzyme inhibitors*

PBMCs were isolated by standard density gradient separation using Pancoll (PAN Biotech). The differentiation of human B cells to Ab-secreting cells was essentially done as described previously (34–36). PBMCs were seeded at $1 \times 10^6$ cells/ml, stimulated with IL-2 (1000 IU/ml; R&D Systems) and R848 (2.5 μg/ml; Sigma-Aldrich) in RPMI 1640 supplemented with 10% FCS (MilliporeSigma) and penicillin-streptomycin (Life Technologies). After 3 d, PBMCs were washed and seeded at a concentration of $2 \times 10^6$ cells/ml, and after an additional 5 d, supernatants were collected. Secreted IgG was quantified by ELISA (Mabtech, Nacka Strand, Sweden). The human lymphoma cell lines Raji (CCL-86; American Type Culture Collection [ATCC]), which releases TACI (17), and JK-6L (kindly provided by Dr. Silke Meister, Erlangen) (37), which releases sBCMA (25), were cultured in RPMI 1640 media (Sigma-Aldrich) supplemented with 10% FCS and penicillin-streptomycin. For culture of JK-6L, IL-6 (2.5 ng/ml; BioTechne GmbH) was added. Furthermore, for specific analysis of γ-secretase-mediated shedding (25), HEK 293T (CRL-3216; ATCC) or HeLa (CRM-CCL-2; ATCC) cells were transiently transfected using Lipofectamine 2000 (11668019; Thermo

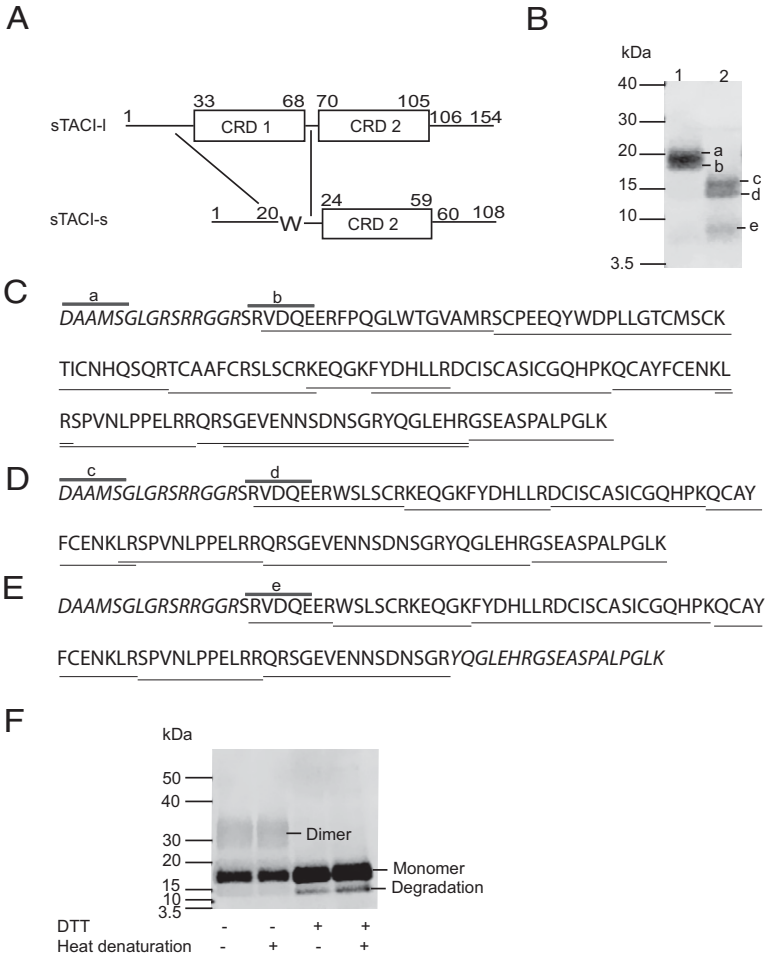


**FIGURE 1.** Analysis of recombinant sTACI-l and sTACI-s. (**A**) Illustration of sTACI-l and sTACI-s adapted from (30). Numbers correspond to amino acid residues of TACI present in recombinant sTACI-l and sTACI-s (23). (**B**) sTACI-l (lane 1) and sTACI-s (lane 2) were separated by SDS-PAGE and visualized by Coomassie blue staining. Bands indicated with a–e were cut and analyzed by mass spectrometry after digestion with trypsin and by N-terminal sequencing (after protein transfer to polyvinylidene difluoride membrane, Coomassie blue staining, and consecutive cutting). (**C**–**E**) Amino acid sequences obtained by mass spectrometry are shown, and peptides identified are underlined. Portions of sTACI-l (C) and sTACI-s (D, E) that were not detected by mass spectrometry are indicated with italic letters. Major sequences obtained by N-terminal sequencing of bands a–e are indicated with a gray line. The initial DAA is vector derived. (**F**) sTACI-l was treated with heat denaturation at 95°C for 5 min, DTT, or both and compared with nontreated sTACI-l. The dimer, monomer, and degradation product of sTACI-l are indicated. Coomassie blue–stained SDS-PAGE was used for analysis.

Fisher Scientific) with BCMA, TACI-l, or TACI-s (in pcDNA3.1). To transfect HEK293T cells, 10 μg DNA per $3 \times 10^6$ cells was applied. To transfect HeLa cells, 14 μg DNA per $2 \times 10^6$ cells was applied. Metalloproteases were inhibited with TAPI-1 (EMD Chemicals/Calbiochem, Gibbstown, NJ) for a disintegrin and metalloproteinase domain-containing protein 10 (ADAM10) and ADAM17. GI254023X (Sigma-Aldrich) was used to specifically block ADAM10. The following γ-secretase inhibitors were used: (2S)-N-[(3,5-Difluorophenyl)acetyl]-L-alanyl-2-phenyl]glycine 1,1-dimethylethyl ester (DAPT) (Calbiochem Merck, Darmstadt, Germany), DAPT GSI-IX (Absource Diagnostics GmbH, Munich, Germany), L685458 (R&D Systems), RO4929097 (Absource Diagnostics), and the stereoisomer SSR of LY-411575, referred to as LY-411575-I (Sigma-Aldrich). Corresponding volumes of DMSO (Sigma-Aldrich) were used as vehicle controls. Cells were treated with different inhibitors for 24 h at the indicated concentrations, and supernatants were harvested to evaluate shedding by ELISA. sTACI was detected by Human TACI/TNFRSF13B DuoSet ELISA, and sTACI-s and sTACI-l were detected as described above. sBCMA was quantified using the Human BCMA/TNFRSF17 DuoSet ELISA (BioTechne GmbH).

### *Statistics*

Prism version 8.0 software (GraphPad Software) was used for analysis. Statistical significance was assessed by paired two-tailed *t* test and Mann-Whitney *U* test. $*p < 0.05$ and $**p < 0.005$ were considered significant.

## Results

### *Characterization of recombinant sTACI-l and sTACI-s*

sTACI-l has two CRDs (CRD1 and CRD2), whereas sTACI-s has only one (CRD2) (Fig. 1A). We expressed both proteins recombinantly and pooled 14 independent purifications for sTACI-l and 5 independent purifications for sTACI-s. We produced pure but heterogeneous proteins as judged from Coomassie blue–stained SDS-PAGE gels under reducing conditions. The recombinant proteins were analyzed by mass spectrometry and N-terminal sequencing (Fig. 1B–1E). Coomassie staining (Fig. 1B) showed that both sTACI-l and sTACI-s migrated as doublet or broad bands. N-terminal sequencing of the excised upper bands yielded mainly the predicted mature N-terminal sequence of these constructs (DAAMS), whereas the lower bands yielded mainly sequences starting with Ser13 of TACI (SRVDQE) (Fig. 1C, 1D). This is consistent with furin-mediated cleavage after Arg12 in the sequence Arg9-Gly10-Gly11-Arg12. Indeed, furin is a major protease of the secretory pathway primarily located at the Golgi apparatus that cleaves proteins after basic residues in motifs such as Arg-X-X-Arg, Arg-X-Lys/Arg-Arg, or Lys/Arg-X-X-X-Lys/Arg-Arg (38). Tryptic digests

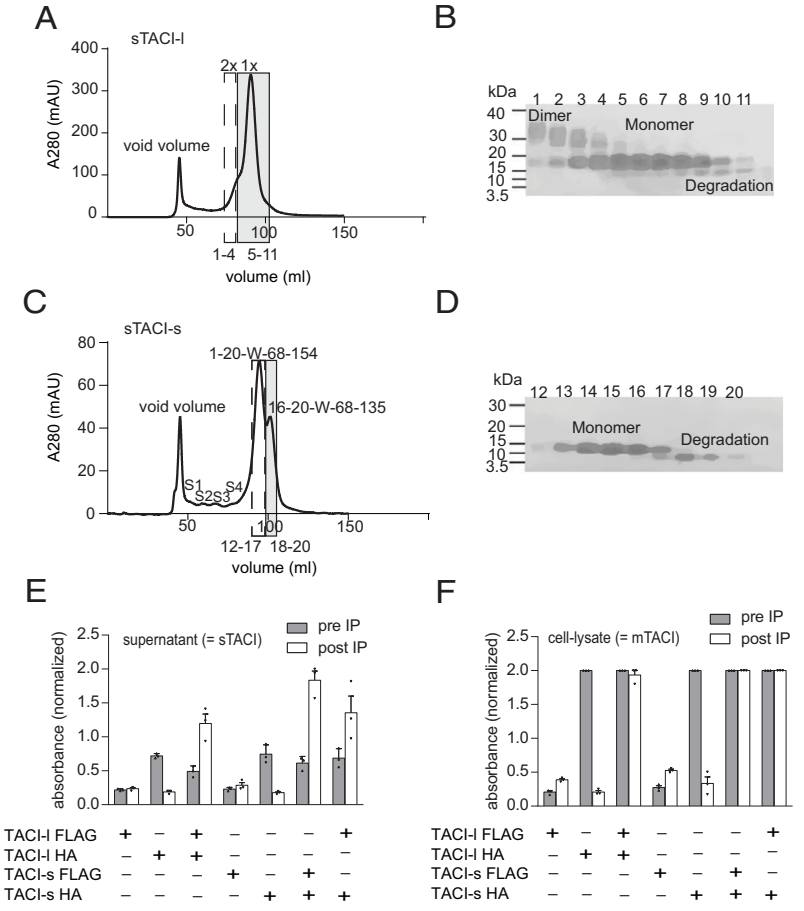


**FIGURE 2.** Oligomerization of TACI-l and TACI-s. (**A**) SEC UV chromatogram profile of sTACI-l. The sTACI-l monomer is indicated by the inscription 1× and a gray rectangle, and the sTACI-l dimer is indicated by 2× and a rectangle with dotted lines. (**B**) Fractions 1–11 of the SEC (shown in A) were separated by SDS-PAGE under nonreducing conditions and stained with Coomassie blue. (**C**) sTACI-s was analyzed by SEC, and the resulting UV chromatogram is shown. sTACI-s is indicated by the inscription (1-20-W-68-154) and a rectangle with dotted lines, and the degradation product of sTACI-s (16-20-W-68-135) is indicated with a gray rectangle. S1–S4 indicate higher-grade oligomers of sTACI-s (validated by ELISA). (**D**) Fractions 12–20 of the SEC (shown in C) were separated by SDS-PAGE under nonreducing conditions and stained with Coomassie blue. The numbers below the *x*-axis indicate the fractions that were used for Coomassie blue staining. (**E** and **F**) HEK293T cells were cotransfected with TACI-coding plasmids that either contained an HA tag or a Flag tag. Anti-Flag beads were used for co-IP and a sandwich ELISA against the HA tag for detection of protein–protein interactions. The supernatants (E) and cell lysates (F) were harvested 48–72 h after transfection. Small fractions of each condition were saved before Flag immunoprecipitation (IP; pre-IP). The pre- and post-IP samples were then measured by anti-HA ELISA. The different conditions are indicated in the legend below the graph. Pre-IP samples are indicated by gray and post-IP samples by white columns. Supernatant corresponds to soluble TACI (sTACI) and cell-lysate to membrane-bound TACI (=mTACI). Combined data of three independent experiments are shown (mean ± SEM).

of TACI bands followed by mass spectrometric analysis of peptides identified peptides covering aa residues 13–154 of sTACI-l and aa residues 13–108 of sTACI-s (Fig. 1B–1D). A smaller band present in the sTACI-s preparation was identified as starting at Ser13 but lacking the C-terminal tryptic peptide 89–108 (Fig. 1E). sTACI-l appeared at m.w. suggesting that, in addition to the monomeric form, preparations contain also a dimer (Fig. 1F). The reducing agent DTT, but not heat denaturation for 5 min at 95°C, was able to convert sTACI-l dimer into monomers (Fig. 1F). In summary, we produced both sTACI isoforms recombinantly.

*Oligomerization of sTACI-l and sTACI-s*

To study the oligomerization we observed in Fig. 1F, we used SEC and co-IP of tagged proteins. SEC revealed that sTACI-l contains both dimers and monomers (Fig. 2A), which was validated by SDS-PAGE of the different fractions under nonreducing conditions (Fig. 2B). The SEC chromatogram of sTACI-s revealed a major peak of monomers preceded by less abundant putative oligomers of higher m.w. and followed by a smaller peak (Fig. 2C). SDS-PAGE indicated that the two major peaks of sTACI-s consisted of the monomer and the degradation product already characterized in the input (Fig. 2D, Fig. 1E). m.w. estimations revealed that S1–S4 were multimers of sTACI-s (S4 = 3× sTACI-s, S3 = 6× sTACI-s, S2 = 9× sTACI-s, S1 = 12× sTACI-s); these fractions were confirmed to consist of sTACI by ELISA.

We next investigated the oligomerization of TACI-l and TACI-s in both soluble and, as a control, membrane-bound form by co-IP in transfected cells. We specifically tested whether sTACI-s can build oligomers and if there is a direct interaction between both soluble isoforms. TACI constructs with N-terminal HA or Flag tag were immunoprecipitated with anti-Flag M2 magnetic beads. Supernatants were used to evaluate shed sTACI (Fig. 2E) and cell lysates for membrane-bound TACI (Fig. 2F). Both sTACI isoforms built homo-oligomers in soluble and membrane-bound form (Fig. 2E, 2F). Additionally, heteromers of both splice variants formed (Fig. 2E, 2F). Thus, TACI-l and TACI-s build homo- and hetero-oligomers in both soluble and membrane-bound form.

*BAFF and APRIL binding of sTACI-l and sTACI-s*

We analyzed the interaction of sTACI-l and sTACI-s with BAFF and APRIL. We used ELISAs to evaluate the binding capacity and a luciferase-based NF-κB reporter assay to analyze functionality as a decoy receptor. We found that sTACI-l bound significantly better to BAFF than sTACI-s before the assay reached saturation (0.0024–0.3000 nM; Fig. 3A). To an even greater extent, sTACI-l showed a significantly stronger binding capacity for APRIL than sTACI-s over a wide range of concentrations (0.012–1.5000 nM; Fig. 3B). One feature of soluble receptors is their ability to bind to their original ligands as decoy receptors. These interactions prevent ligands from binding to membrane-bound receptors, inhibiting their biological function. Thus, we analyzed the decoy receptor function of sTACI-l and sTACI-s by testing their capacity to prevent BAFF and APRIL stimulation of transfected BCMA. We found that both sTACI-l and sTACI-s similarly inhibited BAFF (Fig. 3C) but that only sTACI-l also blocked APRIL at roughly stoichiometric amounts (Fig. 3D).

Because we observed that sTACI-l appeared as both monomer and dimer, we specifically analyzed how SEC-separated sTACI-l monomers and dimers bind and inhibit BAFF and APRIL. We found that the monomer and the dimer of sTACI-l bound similarly to BAFF and APRIL, although sTACI-l dimer bound slightly better than the monomer at nonsaturating concentrations until the assay reached saturation (0.0024–0.0600 nM) (Fig. 4A, 4B). Accordingly, sTACI-l monomer and dimer had similar potency to inhibit BAFF and APRIL, although sTACI-l dimer appeared slightly more potent than the monomer (Fig. 4C, 4D). In summary, binding assays by ELISA and NF-κB reporter assays showed that both forms of sTACI block BAFF but that only sTACI-l can additionally block APRIL. No striking difference between sTACI-l monomer and dimer was found.

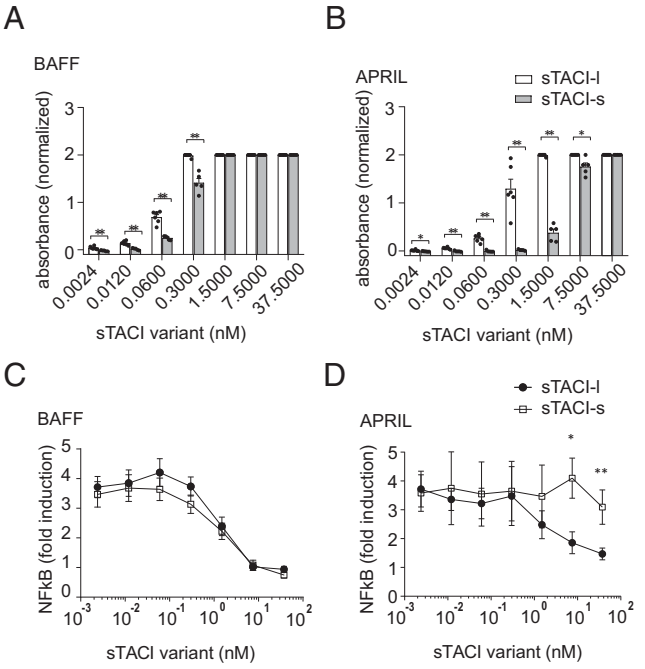


**FIGURE 3.** Binding and decoy activities of sTACI-l and sTACI-s. (**A** and **B**) Plates were coated with the anti-Flag mAb. Flag-tagged ligands (BAFF, APRIL) were added (100 ng/ml), and a dilution series of sTACI-s or sTACI-l was applied. Bound sTACI variants were detected with the anti-TACI detection Ab from the Human TACI/TNFRSF13B DuoSet ELISA. The *y*-axis shows OD 450–OD 540 normalized against the background binding of the used ligand to the plate (normalized against conditions with only BAFF [A] or APRIL [B] added to the coated plates). Combined data of five or six independent experiments (mean ± SEM) are shown. Mann-Whitney *U* test in (B) and (C) (*$p < 0.05$, **$p < 0.005$). (**C** and **D**) HEK293T cells were transfected with BCMA, Renilla luciferase, and NF-κB-driven firefly luciferase. Flag-tagged BAFF (C) and APRIL (D) at a constant concentration of 3 nM were added to the transfected cells in the presence of a dilution series of either sTACI-l or sTACI-s (0.0024–37.5 nM). The concentration of the sTACI isoforms is shown on the *x*-axis, and the NF-κB fold induction is shown on the *y*-axis. Mann-Whitney *U* test in (C) (*$p < 0.05$, **$p < 0.005$). Combined data of six independent experiments are shown (mean ± SEM).

*Validation of isoform-specific ELISAs*

First, we evaluated whether we can detect both recombinantly produced sTACI isoforms using a commercially available TACI ELISA kit and found that the kit detected both isoforms over a wide range of concentrations (50–10,000 pg/ml) (Fig. 5A). Clone B10 (Fig. 5B) and the commercially available clone 3H11 (Fig. 5C) were selected to detect sTACI-l, and clone 9C5 was selected to detect sTACI-s (Fig. 5D, 5E). Overnight incubation increased the sensitivity of the sTACI-s (Fig. 5E). The isoform-specific Abs detected their corresponding sTACI isoform over a wide range of concentrations (100–10,000 pg/ml) (Fig. 5B–5D). Only clone B10 showed cross-reactivity for sTACI-s at high concentration (5,000–10,000 pg/ml), whereas the clone 11H3 remained sTACI-l specific at these high concentrations (Fig. 5C). In summary, the clones B10, 11H3, and 9C5 can be used in ELISA-based assays to differentiate between sTACI-l and sTACI-s.

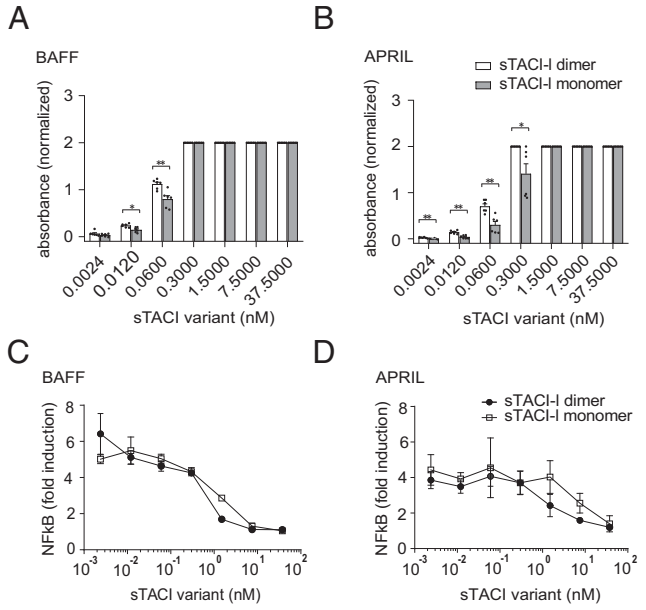


**FIGURE 4.** Effects of dimerization of TACI-l on binding and decoy activities. sTACI-l monomers and dimers were separated by SEC (see Fig. 3), and their concentrations were determined by ELISA. The separated fractions were analyzed for binding to BAFF and APRIL (**A** and **B**) and for decoy activity blocking BAFF and APRIL (**C** and **D**). (A and B) Plates were coated with anti-Flag mAb. Flag-tagged BAFF or APRIL was added (3 nM) in the presence of a dilution series of the sTACI-l dimers or monomers. The OD values OD450−OD540 normalized against the background binding of the used ligand to the plate (normalized against conditions with only BAFF [A] or APRIL [B] added to the coated plates) are displayed. Combined data of six independent experiments (mean ± SEM) are shown. Mann-Whitney *U* test in (B) and (C) (*$p < 0.05$, **$p < 0.005$). (C and D) HEK293T cells were transfected with BCMA, Renilla luciferase, and NF-κB-driven firefly luciferase. Flag-tagged BAFF (C) and APRIL (D) were added at a constant concentration of 3 nM to the transfected cells in the presence of a dilution series of either sTACI-l or sTACI-s (0.0024−37.5 nM). The concentration of the sTACI isoforms is shown on the *x*-axis, and the NF-κB fold induction is shown on the *y*-axis. Combined data of three independent experiments are shown (mean ± SEM).

*Proteases involved in shedding of TACI-l and TACI-s*

First, we used enzyme inhibitors and analyzed the spontaneous release of TACI isoforms by Raji cells. We noted that also these cells released more sTACI-l (267 ± 54 pg/ml) than sTACI-s (126 ± 78 pg/ml). The release of sTACI-l was inhibited by the ADAM10-specific inhibitor GI254023X and to a lesser extent by TAPI-1 (inhibits ADAM10 and ADAM17), but not by the γ-secretase inhibitor DAPT (Fig. 6A). Our data indicated that GI254023X also inhibited shedding of sTACI-s, whereas the γ-secretase-inhibitor DAPT had no effect (Fig. 6B). For comparison, we used the myeloma cell line JK6 that releases sBCMA and also used several γ-secretase inhibitors (Fig. 6C). These experiments confirm our previous observation that sBCMA is released by γ-secretase (25). We additionally investigated the release of sTACI from activated human B cells (Supplemental Fig. 1) and found that the shedding of total sTACI and of the prevalent isoform sTACI-l (Fig. 7A) was inhibited by GI254023X. Because the absolute amounts of sTACI-s in these experiments were rather low, and because TACI-s, like BCMA, contains a single CRD, we analyzed the potential impact of the γ-secretase in further experiments thoroughly comparing the shedding of BCMA, TACI-s, and TACI-l. We transiently transfected BCMA, TACI-s, and TACI-l into HEK293T (Fig. 6D−6F) or HeLa cells (Fig. 6G−6I). Because γ-secretase is ubiquitously expressed, these cell culture systems have proven value to identify substrates of γ-secretase (25). We used several known γ-secretase inhibitors. Both cell culture systems with HeLa and HEK cells yielded the same results. The shedding of TACI-l (Fig. 6D, 6G) and TACI-s (Fig. 6E, 6H) was not blocked by inhibiting γ-secretase, in contrast to the shedding of BCMA (Fig. 6F, 6I). Collectively, these experiments indicate that sTACI-s is released by ADAM10 and not by γ-secretase.

*sTACI-l is the prevalent isoform in human serum*

TACI expression on the cell surface is induced when B cells differentiate into plasmablasts (17). Here, we analyzed whether both TACI isoforms are shed from activated B cells. PBMCs from three different healthy donors (Supplemental Table I) were activated with R848 and IL-2, which resulted in plasmablast differentiation with detection of IgG in the supernatant (35, 36). We found that both sTACI-l and sTACI-s are shed from human plasmablasts and noted that sTACI-l is ∼10 times more abundant than sTACI-s (Fig. 7A). Next, we analyzed the presence of sTACI isoforms in serum. We thereby found that the level of sTACI-l was similar to the level of total sTACI (Fig. 7B). Furthermore, we studied if vaccination enhanced the level of sTACI in serum. To this end, we analyzed 12 sample pairs pre- and postvaccination (12−20 d after vaccination with the mRNA vaccine from BioNTech [BNT162b2]). We found that sTACI (Fig. 7C) and sTACI-l (Fig. 7D) levels were not significantly increased postvaccination. Thus, activation of Ag-specific B cells after vaccination (39) did not enhance the total level of sTACI in serum. Together, this part of our analysis showed that sTACI-l is the predominant isoform secreted by primary plasmablasts as well as the prevalent isoform in human serum.

## Discussion

In this study, we identified and characterized the two splice variants of human TACI in soluble form. We show that both isoforms are released by primary human plasmablasts and the lymphoma cell line Raji. sTACI-l is the predominant isoform secreted in vitro and also in human serum. We provide insights into the mechanism behind their shedding and characterize their decoy activity as well as oligomerization status.

The proteolytic ectodomain shedding of membrane proteins in mammals is a key cellular mechanism to control the abundance and activation of membrane receptors and to release decoys (40, 41). This shedding can be executed by proteases of different families, such as ADAM and β-site amyloid precursor protein cleaving enzyme family proteases and intramembrane or soluble proteases (42). Previous work has revealed different proteolytic mechanisms mediating the shedding of BAFF/APRIL receptors (27). BCMA is directly shed by γ-secretase (25), a ubiquitous intramembrane protease for type I−oriented membrane proteins with N-termini present on the extracellular side, as is the case for BCMA, BAFF-R, and TACI. BAFF-R is shed by ADAM10 and ADAM17 when BAFF has bound to TACI (26). TACI has been investigated as the long isoform TACI-l, and it was found to be shed by ADAM10 independent of ligand binding followed by the processing of the membrane stub by γ-secretase (17). The shedding of TACI-l by ADAM10 is confirmed in this study. The shedding of TACI-s has not been evaluated so far. BCMA was previously identified as the first natural membrane protein to be directly shed by γ-secretase (25). The precise identification of receptors for BAFF and APRIL that are cleaved or not by γ-secretase is of relevance, because a therapeutic approach combining anti-BCMA with inhibition of γ-secretase is currently in clinical evaluation (7). Because TACI-s has a single

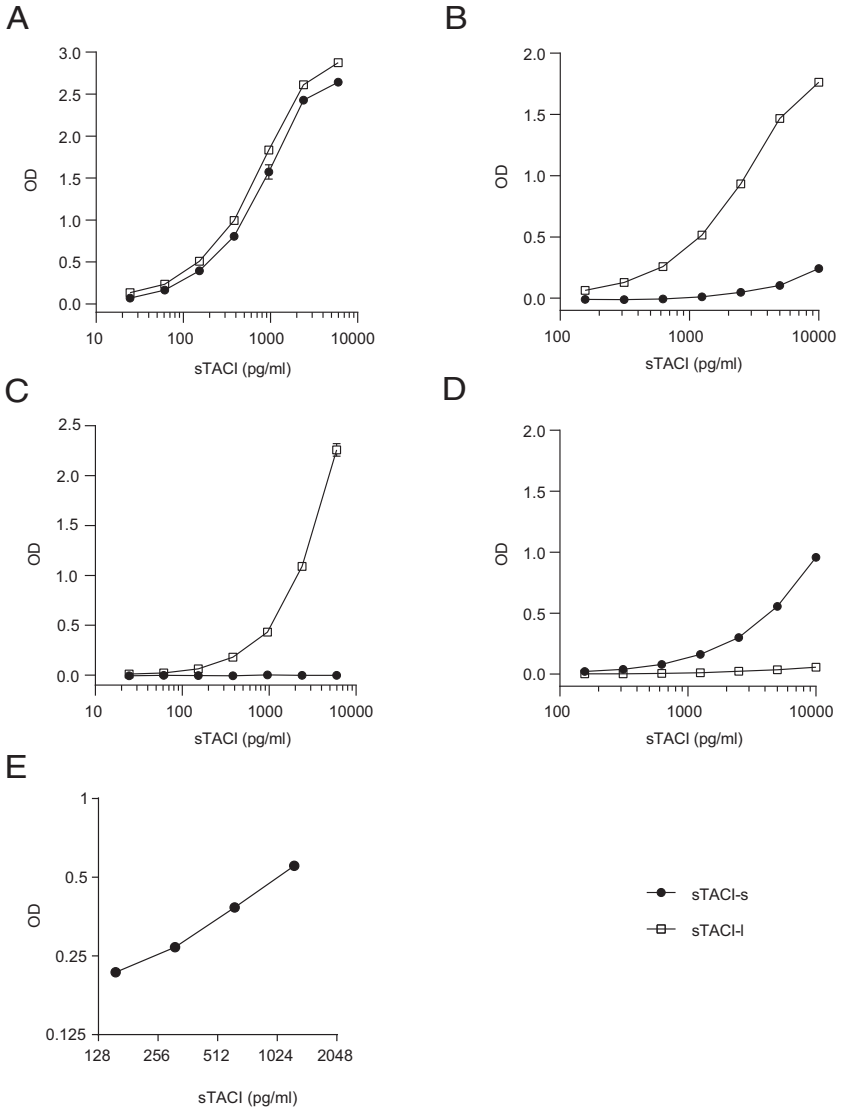


**FIGURE 5.** Validation of sTACI isoform-specific ELISAs. (**A**) Both sTACI-l and sTACI-s were detected by the commercially available Human TACI/TNFRSF13B DuoSet ELISA kit (DY174). (**B**–**E**) To detect sTACI isoforms, ELISA plates were coated with the TACI-l-specific mAb B10 (B), the coating mAb from DY174 DuoSet kit (C), or the TACI-s-specific mAb 9C5 (D and E). sTACI-l or sTACI-s was added at the indicated concentrations and incubated for 2 h (A–D) or overnight (E). The ELISAs were developed with biotinylated anti-TACI (R&D Systems) (B, D and E), which recognizes both TACI-l and TACI-s or the TACI-l-specific biotinylated 11H3 (C). Absorbance was measured (absorbance 450−540), and the background of the blank was subtracted (OD; *y*-axis).

extracellular CRD, like BCMA, it was a candidate for shedding by γ-secretase. Our data indicate that not only the long but also the short isoform of TACI is shed by ADAM10 and not by γ-secretase, like BCMA. It is known that the shedding by γ-secretase is heavily influenced by the length of the extracellular part of the substrate; cleavage of proteins with an extracellular domain fewer than ∼100 aa were cleaved by γ-secretase with much greater efficiency (43). Doubling of the extracellular part of BCMA from 54 aa to 108 aa largely abrogated the shedding by γ-secretase (25). We assume that the total length of the extracellular part of sTACI-s with 119 aa is the reason why it is not directly processed by γ-secretase.

We found that both isoforms of TACI were spontaneously shed from activated human B cells, with sTACI-l being much more abundant than sTACI-s. Shed soluble receptors add another layer of complexity to the BAFF/APRIL system because they can capture the ligands and prevent them from binding to the membrane-bound receptors. We had previously reported that sTACI functions as such a decoy for BAFF and APRIL, but we could not differentiate in that study between the two isoforms (17). Therefore, we investigated whether both soluble isoforms can be decoys for BAFF and APRIL. The present study reveals differences in ligand binding between the two soluble isoforms of TACI. Although sTACI-l and sTACI-s bound BAFF similarly, sTACI-l was superior in APRIL binding. We observed this difference in both binding and NF-κB reporter assays. We went on to analyze the linkage between the extracellular domain structure, oligomerization, and decoy activity in detail. Oligomerization is a prominent feature of many components of the BAFF/APRIL system. BAFF and APRIL assemble as trimers (44–46), just like TNF and other TNF ligand superfamily members (47). TACI-l builds oligomers in soluble and membrane-bound form (17). TACI-s builds oligomers in membrane-bound form (homo-oligomers) and interacts with TACI-l as well (hetero-oligomers) (31). TACI-l contains, in contrast to TACI-s, the CRD1 domain, which is proposed to facilitate oligomerization (24). In line with this, we found that sTACI-l showed a higher degree of oligomerization than sTACI-s. We noted that dimers of sTACI-l have only

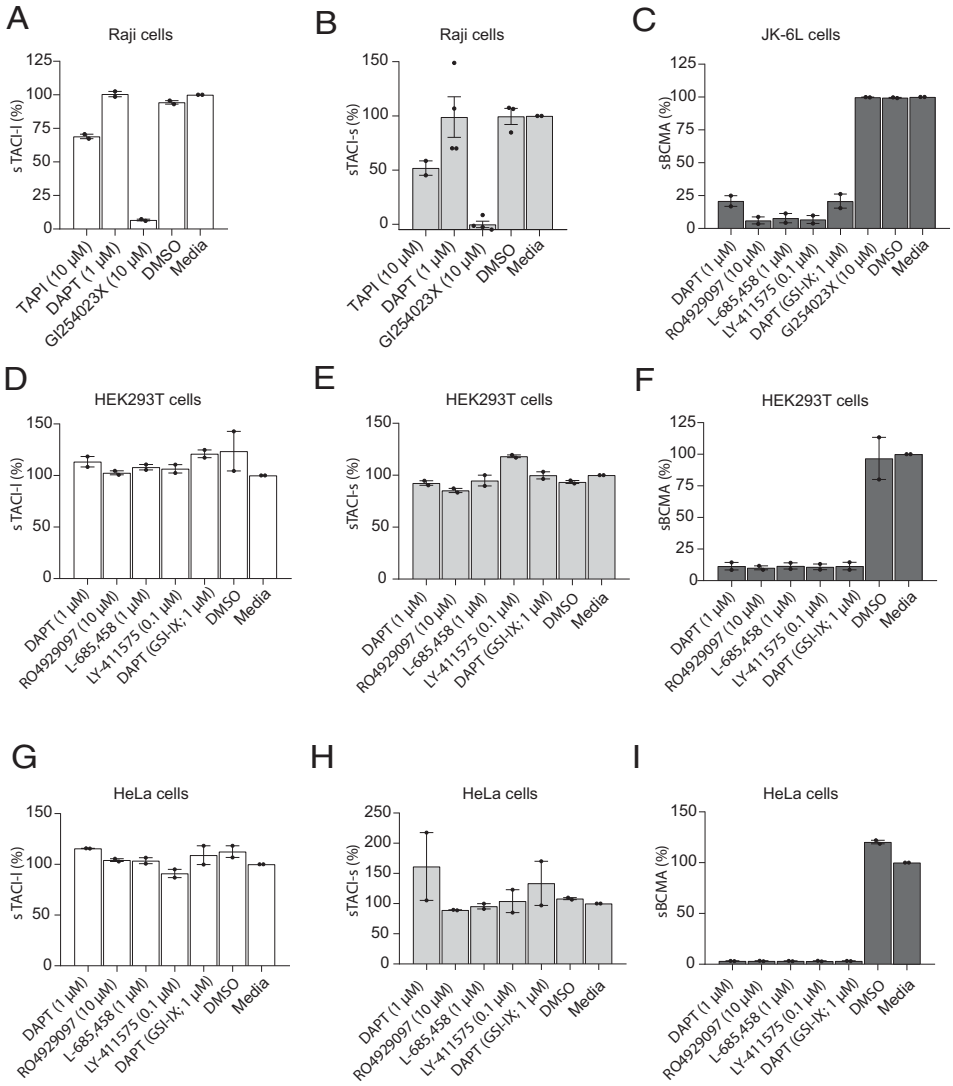


**FIGURE 6.** Proteases releasing sTACI-l, sTACI-s, and sBCMA. Raji (**A** and **B**) and JK-6L cells (**C**) were treated with the indicated enzyme inhibitors for 24 h. The released sTACI-l (white columns), sTACI-s (light gray columns), and sBCMA (dark gray columns) were quantified by ELISA and normalized to untreated cells. HEK293T cells (**D**–**F**) and HeLa cells (**G**–**I**) were transiently transfected with TACI-l (D and G), TACI-s (E and H), or BCMA (F and I). Cells were treated with the indicated inhibitors for 24 h, and supernatants were harvested to evaluate shedding by ELISA. Combined data of two to four independent experiments are shown (mean ± SEM). The values in culture medium without inhibitors were set to 100%, and the effects of the inhibitors were calculated in relation to the noninhibitor (culture medium–only) control.

a slightly higher binding and decoy activity than monomeric sTACI-l. This part of our study suggests that the presence of both CRD1 and CRD2 in sTACI-l specifically increases its binding and decoy activity for APRIL. (Hetero-)oligomers of BAFF and APRIL have been characterized in vivo (48, 49). Oligomerization seems to be of functional relevance for membrane-bound TACI (50), and future studies will show whether the oligomers of soluble TACI isoforms are of biological significance.

sTACI might be a useful biomarker in inflammatory diseases and certain B cell–derived malignancies. In systemic lupus erythematosus, sTACI is elevated in serum (17, 51, 52) and might correlate with disease activity (17, 52). In rheumatoid arthritis, elevated levels of APRIL and sBCMA, but not of sTACI, were observed (53). In neuroinflammatory diseases such as MS and neuroborreliosis, sTACI is elevated in the cerebrospinal fluid and reflects local IgG production, which further indicates a relevant role of Ab-secreting cells in releasing sTACI (10, 17, 27). TACI, however, is expressed not only by Ab-secreting cells but also by a subset of memory B cells, marginal zone B cells, and B1 cells (54). Nevertheless, Ab-secreting cells are major contributors to sTACI release (17, 55).

B cell–depleting therapy with anti-CD20 in MS reduces unbound sTACI in serum and spinal fluid due to increased complex formation with BAFF (56); it is tempting to speculate that this reduction of sTACI is beneficial in MS, because the application of sTACI (atacicept) unexpectedly worsened MS (11). In an oncological setting, primary CNS lymphoma, sTACI is a biomarker useful for initial diagnosis and also therapy responses (18). We present here specific ELISAs that distinguish sTACI-s and sTACI-l. We found that sTACI-l is the predominant isoform in serum and that vaccination did not significantly increase sTACI and sTACI-l levels. These isoform-specific ELISAs offer the possibility to improve the utility of sTACI-l as a biomarker in lymphoma and autoimmune diseases, but further studies are needed to evaluate the relevance of sTACI-s.

Collectively, we present tools that distinguish two isoforms of sTACI and show that both were spontaneously released from

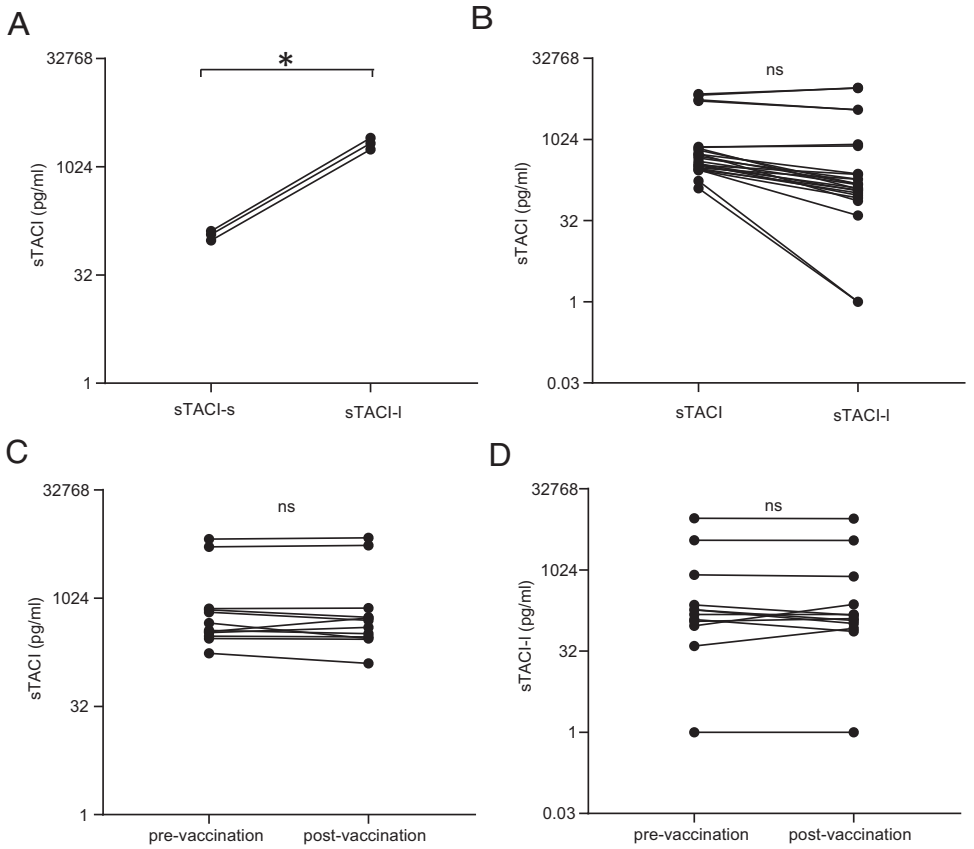


**FIGURE 7.** TACI-l is the predominant isoform released by plasmablasts in vitro and also in serum. (**A**) PBMCs from three healthy control subjects were differentiated into plasmablasts. sTACI-l and sTACI-s were detected with isoform-specific ELISAs. (**B**) Evaluation of sTACI-l and sTACI levels in healthy control subjects in serum samples prevaccination and 12–20 d postvaccination with the BioNTech mRNA vaccine. (**C** and **D**) Comparison of sTACI (C) or sTACI-l levels (D) pre- and postvaccination. The *y*-axis is shown as $\log_2$ scale. Values obtained from the same cell culture supernatant (A), serum (B), or samples from the same individual pre- and postvaccination (C and D) are connected. Paired two-tailed t-test (* $p < 0.05$). ns, not significant.

activated human B cells, with a predominance of sTACI-l. sTACI-l is also the dominant isoform in human serum. Both TACI-l and TACI-s are shed by ADAM10, although TACI-s comprises only one CRD like BCMA, which is directly shed by γ-secretase. sTACI-l and sTACI-s acted as decoy receptors for BAFF, but only sTACI-l also efficiently inhibited APRIL. Although sTACI-s was mainly monomeric, sTACI-l also formed dimers whose binding and decoy activities were slightly higher than, but not fundamentally different from, those of the monomers. Thus, we provide new insights into the complexity of the BAFF/APRIL system, which is a therapeutic target in hemato-oncology and autoimmune diseases.

## Acknowledgments

We are grateful to Drs. Anneli Peters and Naoto Kawakami for comments on the manuscript. We thank Eva Oswald and Dr. Stephan Winklmeier for valuable support.

## Disclosures

M.L.F. has received speaker's honoraria by Alexion, received a Scientific Progress Immunoglobulins in Neurology award from Grifols, and is a member of the Alexion-Akademie since 2022 outside the submitted work. T.K. has served on advisory boards for Roche Pharma and has received personal compensations/speaker honoraria from Bayer Healthcare, Teva Pharma, Merck, NovartiPharma, Sanofi-Aventis/Genzyme, Roche Pharma, and Biogen and grant support from Novartis and Chugai Pharma. F.S.T. received grant support from Novartis Pharma GmbH. E.M. received personal compensations/speaker honoraria from Roche, Novartis, Sanofi, TEVA, Biogen, Bioeq, and Merck and research support from Novartis, Sanofi, Merck, Roche, and GlycoEra. These competing interests played no role in the research design, reference collection, decision to publish, or preparation of the manuscript. The other authors have no financial conflicts of interest.

## References

1. Samy, E., S. Wax, B. Huard, H. Hess, and P. Schneider. 2017. Targeting BAFF and APRIL in systemic lupus erythematosus and other antibody-associated diseases. *Int. Rev. Immunol.* 36: 3–19.
2. Mackay, F., and P. Schneider. 2009. Cracking the BAFF code. *Nat. Rev. Immunol.* 9: 491–502.
3. Stohl, W., J. L. Scholz, and M. P. Cancro. 2011. Targeting BLyS in rheumatic disease: the sometimes-bumpy road from bench to bedside. *Curr. Opin. Rheumatol.* 23: 305–310.
4. Lee, L., B. Draper, N. Chaplin, B. Philip, M. Chin, D. Galas-Filipowicz, S. Onuoha, S. Thomas, V. Baldan, R. Bughda, et al. 2018. An APRIL-based chimeric antigen receptor for dual targeting of BCMA and TACI in multiple myeloma. *Blood* 131: 746–758.
5. Cohen, A. D., A. L. Garfall, E. A. Stadtmauer, J. J. Melenhorst, S. F. Lacey, E. Lancaster, D. T. Vogl, B. M. Weiss, K. Dengel, A. Nelson, et al. 2019. B cell maturation antigen-specific CAR T cells are clinically active in multiple myeloma. *J. Clin. Invest.* 129: 2210–2221.
6. Raje, N., J. Berdeja, Y. Lin, D. Siegel, S. Jagannath, D. Madduri, M. Liedtke, J. Rosenblatt, M. V. Maus, A. Turka, et al. 2019. Anti-BCMA CAR T-cell therapy bb2121 in relapsed or refractory multiple myeloma. *N. Engl. J. Med.* 380: 1726–1737.
7. Pont, M. J., T. Hill, G. O. Cole, J. J. Abbott, J. Kelliher, A. I. Salter, M. Hudecek, M. L. Comstock, A. Rajan, B. K. R. Patel, et al. 2019. γ-Secretase inhibition increases efficacy of BCMA-specific chimeric antigen receptor T cells in multiple myeloma. *Blood* 134: 1585–1597.
8. Demel, I., J. R. Bago, R. Hajek, and T. Jelinek. 2021. Focus on monoclonal antibodies targeting B-cell maturation antigen (BCMA) in multiple myeloma: update 2021. *Br. J. Haematol.* 193: 705–722.
9. Shah, N., A. Chari, E. Scott, K. Mezzi, and S. Z. Usmani. 2020. B-cell maturation antigen (BCMA) in multiple myeloma: rationale for targeting and current therapeutic approaches. *Leukemia* 34: 985–1005.

10. Meinl, E., and M. Krumbholz. 2021. Endogenous soluble receptors sBCMA and sTACI: biomarker, immunoregulator and hurdle for therapy in multiple myeloma. *Curr. Opin. Immunol.* 71: 117–123.
11. Kappos, L., H. P. Hartung, M. S. Freedman, A. Boyko, E. W. Radü, D. D. Mikol, M. Lamarine, Y. Hyvert, U. Freudensprung, T. Plitz, and J. van Beek; ATAMS Study Group. 2014. Atacicept in multiple sclerosis (ATAMS): a randomised, placebo-controlled, double-blind, phase 2 trial. *Lancet Neurol.* 13: 353–363.
12. Rojas, O. L., A. K. Pröbstel, E. A. Porfilio, A. A. Wang, M. Charabati, T. Sun, D. S. W. Lee, G. Galicia, V. Ramaglia, L. A. Ward, et al. 2019. Recirculating intestinal IgA-producing cells regulate neuroinflammation via IL-10. [Published erratum appears in 2019 *Cell* 177: 492–493.] *Cell* 176: 610–624.e18 .
13. Pröbstel, A. K., X. Zhou, R. Baumann, S. Wischnewski, M. Kutza, O. L. Rojas, K. Sellrie, A. Bischof, K. Kim, A. Ramesh, et al. 2020. Gut microbiota-specific $IgA^+$ B cells traffic to the CNS in active multiple sclerosis. *Sci. Immunol.* 5: eabc7191.
14. Fehres, C. M., N. O. van Uden, N. G. Yeremenko, L. Fernandez, G. Franco Salinas, L. M. van Duivenvoorde, B. Huard, J. Morel, H. Spits, M. Hahne, and D. L. P. Baeten. 2019. APRIL induces a novel subset of $IgA^+$ regulatory B cells that suppress inflammation via expression of IL-10 and PD-L1. *Front. Immunol.* 10: 1368.
15. Baert, L., M. Benkhoucha, N. Popa, M. C. Ahmed, B. Manfroi, J. Boutonnat, N. Sturm, G. Raguenez, M. Tessier, O. Casez, et al. 2019. A proliferation-inducing ligand-mediated anti-inflammatory response of astrocytes in multiple sclerosis. *Ann. Neurol.* 85: 406–420.
16. Pracht, K., J. Meinzinger, P. Daum, S. R. Schulz, D. Reimer, M. Hauke, E. Roth, D. Mielenz, C. Berek, J. Côrte-Real, et al. 2017. A new staining protocol for detection of murine antibody-secreting plasma cell subsets by flow cytometry. *Eur. J. Immunol.* 47: 1389–1392.
17. Hoffmann, F. S., P. H. Kuhn, S. A. Laurent, S. M. Hauck, K. Berer, S. A. Wendlinger, M. Krumbholz, M. Khademi, T. Olsson, M. Dreyling, et al. 2015. The immunoregulator soluble TACI is released by ADAM10 and reflects B cell activation in autoimmunity. *J. Immunol.* 194: 542–552.
18. Thaler, F. S., S. A. Laurent, M. Huber, M. Mulazzani, M. Dreyling, U. Ködel, T. Kümpfel, A. Straube, E. Meinl, and L. von Baumgarten. 2017. Soluble TACI and soluble BCMA as biomarkers in primary central nervous system lymphoma. *Neuro-oncol.* 19: 1618–1627.
19. Xu, S., and K. P. Lam. 2020. Transmembrane activator and CAML interactor (TACI): another potential target for immunotherapy of multiple myeloma? *Cancers (Basel)* 12: 1045.
20. Eslami, M., E. Meinl, H. Eibel, L. Willen, O. Donzé, O. Distl, H. Schneider, D. E. Speiser, D. Tsiantoulas, Ö. Yalkinoglu, et al. 2020. BAFF 60-mer, and differential BAFF 60-mer dissociating activities in human serum, cord blood and cerebrospinal fluid. *Front. Cell Dev. Biol.* 8: 577662.
21. Salzer, U., and B. Grimbacher. 2021. TACI deficiency - a complex system out of balance. *Curr. Opin. Immunol.* 71: 81–88.
22. Salzer, U., H. M. Chapel, A. D. Webster, Q. Pan-Hammarström, A. Schmitt-Graeff, M. Schlesier, H. H. Peter, J. K. Rockstroh, P. Schneider, A. A. Schäffer, et al. 2005. Mutations in TNFRSF13B encoding TACI are associated with common variable immunodeficiency in humans. *Nat. Genet.* 37: 820–828.
23. Hymowitz, S. G., D. R. Patel, H. J. Wallweber, S. Runyon, M. Yan, J. Yin, S. K. Shriver, N. C. Gordon, B. Pan, N. J. Skelton, et al. 2005. Structures of APRIL-receptor complexes: like BCMA, TACI employs only a single cysteine-rich domain for high affinity ligand binding. *J. Biol. Chem.* 280: 7218–7227.
24. Garibyan, L., A. A. Lobito, R. M. Siegel, M. E. Call, K. W. Wucherpfennig, and R. S. Geha. 2007. Dominant-negative effect of the heterozygous C104R TACI mutation in common variable immunodeficiency (CVID). *J. Clin. Invest.* 117: 1550–1557.
25. Laurent, S. A., F. S. Hoffmann, P. H. Kuhn, Q. Cheng, Y. Chu, M. Schmidt-Supprian, S. M. Hauck, E. Schuh, M. Krumbholz, H. Rübsamen, et al. 2015. γ-Secretase directly sheds the survival receptor BCMA from plasma cells. *Nat. Commun.* 6: 7333.
26. Smulski, C. R., P. Kury, L. M. Seidel, H. S. Staiger, A. K. Edinger, L. Willen, M. Seidl, H. Hess, U. Salzer, A. G. Rolink, et al. 2017. BAFF- and TACI-dependent processing of BAFFR by ADAM proteases regulates the survival of B cells. *Cell Rep.* 18: 2189–2202.
27. Meinl, E., F. S. Thaler, and S. F. Lichtenthaler. 2018. Shedding of BAFF/APRIL receptors controls B cells. *Trends Immunol.* 39: 673–676.
28. Sanchez, E., E. J. Smith, M. A. Yashar, S. Patil, M. Li, A. L. Porter, E. J. Tanenbaum, R. E. Schlossberg, C. M. Soof, T. Hekmati, et al. 2018. The role of B-cell maturation antigen in the biology and management of, and as a potential therapeutic target in, multiple myeloma. *Target. Oncol.* 13: 39–47.
29. Kyrtsonis, M. C., K. Sarris, E. Koulieris, D. Maltezas, E. Nikolaou, M. K. Angelopoulou, V. Bartzis, T. Tzenou, M. Dimou, M. P. Siakandaris, et al. 2014. Serum soluble TACI, a BLyS receptor, is a powerful prognostic marker of outcome in chronic lymphocytic leukemia. *BioMed Res. Int.* 2014: 159632.
30. Garcia-Carmona, Y., M. Cols, A. T. Ting, L. Radigan, F. J. Yuk, L. Zhang, A. Cerutti, and C. Cunningham-Rundles. 2015. Differential induction of plasma cells by isoforms of human TACI. [Published erratum appears in 2019 *Blood* 134: 843.] *Blood* 125: 1749–1758.
31. Garcia-Carmona, Y., A. T. Ting, L. Radigan, S. K. Athuluri Divakar, J. Chavez, E. Meffre, A. Cerutti, and C. Cunningham-Rundles. 2018. TACI isoforms regulate ligand binding and receptor function. [Published erratum appears in 2019 *Front. Immunol.* 10: 2772.] *Front. Immunol.* 9: 2125.
32. Perera, N. C., K. H. Wiesmüller, M. T. Larsen, B. Schacher, P. Eickholz, N. Borregaard, and D. E. Jenne. 2013. NSP4 is stored in azurophil granules and released by activated neutrophils as active endoprotease with restricted specificity. *J. Immunol.* 191: 2700–2707.
33. Tiller, T., I. Schuster, D. Deppe, K. Siegers, R. Strohner, T. Herrmann, M. Berenguer, D. Poujol, J. Stehle, Y. Stark, et al. 2013. A fully synthetic human Fab antibody library based on fixed VH/VL framework pairings with favorable biophysical properties. *MAbs* 5: 445–470.
34. Pinna, D., D. Corti, D. Jarrossay, F. Sallusto, and A. Lanzavecchia. 2009. Clonal dissection of the human memory B-cell repertoire following infection and vaccination. *Eur. J. Immunol.* 39: 1260–1270.
35. Thaler, F. S., A. L. Thaller, M. Biljecki, E. Schuh, S. Winklmeier, C. F. Mahler, R. Gerhards, S. Völk, F. Schnorfeil, M. Subklewe, et al. 2019. Abundant glutamic acid decarboxylase (GAD)-reactive B cells in gad-antibody-associated neurological disorders. *Ann. Neurol.* 85: 448–454.
36. Winklmeier, S., M. Schlüter, M. Spadaro, F. S. Thaler, A. Vural, R. Gerhards, C. Macrini, S. Mader, A. Kurne, B. Inan, et al. 2019. Identification of circulating MOG-specific B cells in patients with MOG antibodies. [Published errata appear in 2019 *Neurol. Neuroimmunol. Neuroinflamm.* 7: e647 and 2020 *Neurol. Neuroimmunol. Neuroinflamm.* 8: e938.] *Neurol. Neuroimmunol. Neuroinflamm.* 6: 625.
37. Burger, R., J. Wendler, K. Antoni, G. Helm, J. R. Kalden, and M. Gramatzki. 1994. Interleukin-6 production in B-cell neoplasias and Castleman's disease: evidence for an additional paracrine loop. *Ann. Hematol.* 69: 25–31.
38. Thomas, G. 2002. Furin at the cutting edge: from protein traffic to embryogenesis and disease. *Nat. Rev. Mol. Cell Biol.* 3: 753–766.
39. Lee, F. E., J. L. Halliley, E. E. Walsh, A. P. Moscatiello, B. L. Kmush, A. R. Falsey, T. D. Randall, D. A. Kaminiski, R. K. Miller, and I. Sanz. 2011. Circulating human antibody-secreting cells during vaccinations and respiratory viral infections are characterized by high specificity and lack of bystander effect. *J. Immunol.* 186: 5514–5521.
40. Lichtenthaler, S. F., and E. Meinl. 2020. To cut or not to cut: new rules for proteolytic shedding of membrane proteins. *J. Biol. Chem.* 295: 12353–12355.
41. Levine, S. J. 2008. Molecular mechanisms of soluble cytokine receptor generation. *J. Biol. Chem.* 283: 14177–14181.
42. Lichtenthaler, S. F., M. K. Lemberg, and R. Fluhrer. 2018. Proteolytic ectodomain shedding of membrane proteins in mammals—hardware, concepts, and recent developments. *EMBO J.* 37: e99456.
43. Struhl, G., and A. Adachi. 2000. Requirements for presenilin-dependent cleavage of notch and other transmembrane proteins. *Mol. Cell* 6: 625–636.
44. Wallweber, H. J., D. M. Compaan, M. A. Starovasnik, and S. G. Hymowitz. 2004. The crystal structure of a proliferation-inducing ligand, APRIL. *J. Mol. Biol.* 343: 283–290.
45. Oren, D. A., Y. Li, Y. Volovik, T. S. Morris, C. Dharia, K. Das, O. Galperina, R. Gentz, and E. Arnold. 2002. Structural basis of BLyS receptor recognition. *Nat. Struct. Biol.* 9: 288–292.
46. Karpusas, M., T. G. Cachero, F. Qian, A. Boriack-Sjodin, C. Mullen, K. Strauch, Y. M. Hsu, and S. L. Kalled. 2002. Crystal structure of extracellular human BAFF, a TNF family member that stimulates B lymphocytes. *J. Mol. Biol.* 315: 1145–1154.
47. Bodmer, J. L., P. Schneider, and J. Tschopp. 2002. The molecular architecture of the TNF superfamily. *Trends Biochem. Sci.* 27: 19–26.
48. Roschke, V., S. Sosnovtseva, C. D. Ward, J. S. Hong, R. Smith, V. Albert, W. Stohl, K. P. Baker, S. Ullrich, B. Nardelli, et al. 2002. BLyS and APRIL form biologically active heterotrimers that are expressed in patients with systemic immune-based rheumatic diseases. *J. Immunol.* 169: 4314–4321.
49. Schuepbach-Mallepell, S., D. Das, L. Willen, M. Vigolo, A. Tardivel, L. Lebon, C. Kowalczyk-Quintas, J. Nys, C. Smulski, T. S. Zheng, et al. 2015. Stoichiometry of heteromeric BAFF and APRIL cytokines dictates their receptor binding and signaling properties. *J. Biol. Chem.* 290: 16330–16342.
50. Smulski, C. R., L. Zhang, M. Burek, A. Teixidó Rubio, J. S. Briem, M. P. Sica, E. Sevdali, M. Vigolo, L. Willen, P. Odermatt, et al. 2022. Ligand-independent oligomerization of TACI is controlled by the transmembrane domain and regulates proliferation of activated B cells. *Cell Rep.* 38: 110583.
51. Vincent, F. B., R. Kandane-Rathnayake, R. Koelmeyer, A. Y. Hoi, J. Harris, F. Mackay, and E. F. Morand. 2019. Analysis of serum B cell-activating factor from the tumor necrosis factor family (BAFF) and its soluble receptors in systemic lupus erythematosus. *Clin. Transl. Immunology* 8: e1047.
52. Piantoni, S., F. Regola, S. Masneri, M. Merletti, T. Lowin, P. Airò, A. Tincani, F. Franceschini, L. Andreoli, and G. Pongratz. 2021. Characterization of B- and T-cell compartment and B-cell related factors belonging to the TNF/TNFR superfamily in patients with clinically active systemic lupus erythematosus: baseline BAFF serum levels are the strongest predictor of response to belimumab after twelve months of therapy. *Front. Pharmacol.* 12: 666971.
53. Rodríguez-Carrio, J., M. Alperi-López, P. López, F. J. Ballina-García, and A. Suárez. 2018. Profiling of B-cell factors and their decoy receptors in rheumatoid arthritis: association with clinical features and treatment outcomes. *Front. Immunol.* 9: 2351.
54. Mackay, F., and P. Schneider. 2008. TACI, an enigmatic BAFF/APRIL receptor, with new unappreciated biochemical and biological properties. *Cytokine Growth Factor Rev.* 19: 263–276.
55. Robinson, T., A. Abdelhak, T. Bose, E. Meinl, M. Otto, U. K. Zettl, R. Dersch, H. Tumani, S. Rauer, and A. Huss. 2020. Cerebrospinal fluid biomarkers in relation to MRZ reaction status in primary progressive multiple sclerosis. *Cells* 9: 2543.
56. Ho, S., E. Oswald, H. K. Wong, A. Vural, V. Yilmaz, E. Tüzün, R. Türkoğlu, T. Straub, I. Meinl, F. Thaler, et al. 2023. Ocrelizumab treatment modulates B-cell regulating factors in multiple sclerosis. *Neurol. Neuroimmunol. Neuroinflamm.* 10: e200083.

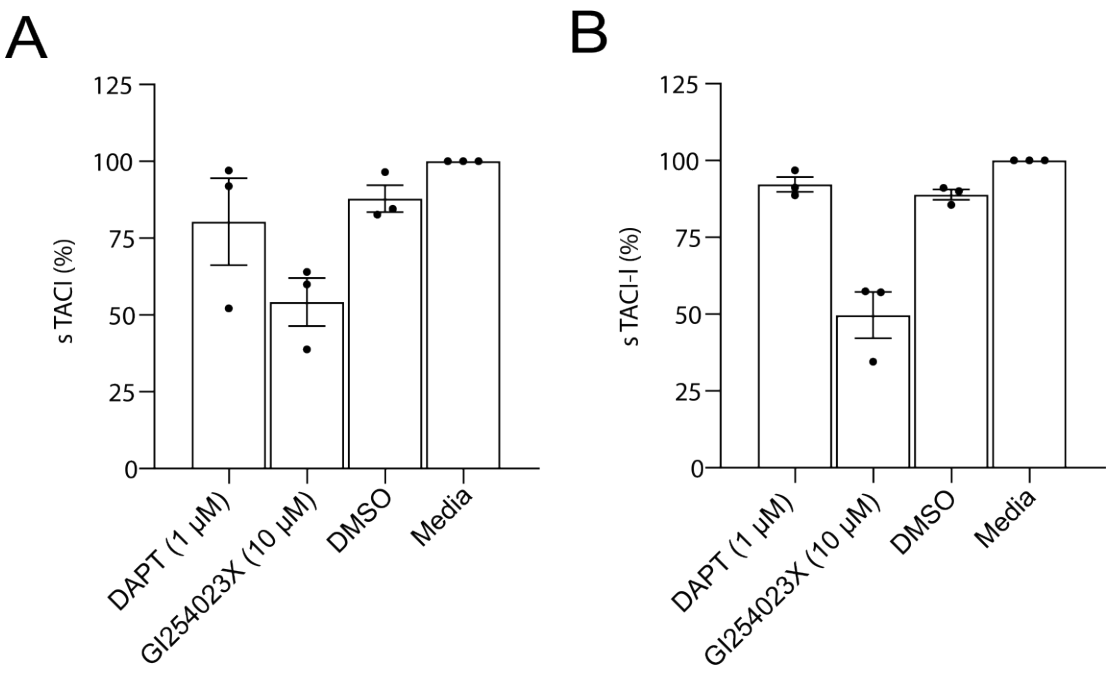


**Figure S1: Proteases releasing sTACI from activated human B cells.**

B cells of three donors were differentiated to plasmablasts and treated with the indicated enzyme inhibitors for 24 h. The released sTACI **(A)** or sTACI-l **(B)** were quantified by ELISA and normalized to untreated cells. Combined data of 3 independent experiments (mean +/- SEM). The values in culture medium without inhibitors were set to 100% and the effects of the inhibitors were calculated in relation to the non-inhibitor (= culture medium only) control.

**Supplementary Table 1. Characteristics and demographics of human specimens**

| Subject ID | Age at TOC; sex (f/m) | Serum | B cells used for activation | Part of vaccination study | Time in days after vaccination with BioNTech mRNA (= post) |
|---|---|---|---|---|---|
| #1 | 32; m | + | - | + | 15 |
| #2 | 58; m | + | - | + | 14 |
| #3 | 23 (= pre) and 24 (= post); f | + | - | + | 16 |
| #4 | 52; f | + | | + | 14 |
| #5 | 32; f | + | - | + | 13 |
| #6 | 27; f | + | - | + | 15 |
| #7 | 26; f | + | | + | 15 |
| #8 | 23; m | + | - | + | 19 |
| #9 | 23; m | + | - | + | 12 |
| #10 | 49; m | + | - | + | 20 |
| #11 | 38; m | + | - | + | 14 |
| #12 | 27; m | + | - | + | 14 |
| HC 15 | 25; m | - | + | - | - |
| HC 19 | 33; f | - | + | - | - |
| HC 28 | 30; m | - | + | - | - |

**Abbreviations:** HC = healthy control; TOC = time of collection